

## Supplementary information

### Efficient electron channel at the TiO<sub>2</sub>/BaTiO<sub>3</sub> nanodots interface for enhanced CO<sub>2</sub> photoreduction

*Yan Huang*<sup>a</sup>, *Wen-fang Zhai*<sup>b</sup>, *Xiao Ying*<sup>c</sup>, *Hao-wen Zhu*<sup>d</sup>, *Rui-tang Guo*<sup>d,\*</sup>,

*Yun-Xiang Pan*<sup>a,\*</sup>

<sup>a</sup> Department of Chemical Engineering, School of Chemistry and Chemical

Engineering, Shanghai Jiao Tong University, 200240, Shanghai, China

<sup>b</sup> Materials Artificial Intelligence Center(MAIC), Shenzhen Institute of Advanced

Technology Chinese Academy of Sciences, 518055, Shenzhen, China

<sup>c</sup> State Key Laboratory of Precision Measurement Technology and Instruments,

Tianjin University, 300072, Tianjin, China

<sup>d</sup> College of Energy and Mechanical Engineering, Shanghai University of Electric Power, 200090

Shanghai, China

**Corresponding author1:** Rui-tang Guo

**Email:** grta@sohu.com

**Corresponding author2:** Yun-xiang Pan

**Email:** yxpan81@sjtu.edu.cn

## Experiment section

**Photocatalytic activity evaluation.** The photocatalytic CO<sub>2</sub> reduction activity was evaluated on an MC-SPB10 system (Merry Change CO., China) under simulating sunlight with a 300W Xe lamp and a 3 AM 1.5 G filter. 99 mL of DI water and 1 ml TEOA dissolved 50 mg of photocatalysts, which was ultrasonicated for 5 min. After vacuuming the reactor, pure CO<sub>2</sub> was introduced and held at 100 kPa for 30 minutes to reach the balance of adsorption-desorption, and then, the light was introduced. The suspension was continuously stirred and kept at 5°C throughout the experimental process. The photocatalytic CO<sub>2</sub> reduction products were analyzed by GCMS-QP2010 SE (SHIMADZU, Japan) using <sup>13</sup>CO<sub>2</sub> for the isotope-labeled experiment.

**Characterization.** The crystalline structures were characterized by XRD (X-ray diffraction, Bruker D8, Cu K $\alpha$  radiation,  $\lambda = 0.154056$  nm). The SEM (scanning electron microscope) and TEM (transmission electron spectroscopy) of the as-prepared photocatalysts were acquired by Phillips XL-30 FEG/NEW and Phillips Model CM200, respectively. The states of the elements were characterized by XPS (X-ray photoelectron spectroscopy) with Al K $\alpha$  radiation sources. The optical adsorption properties of the catalysts were characterized by UV-vis DRS (diffuse reflection spectrum) in the range of 250-800 nm on SHIMADZU UV-3600 (Japan). The presence of oxygen vacancies and superoxide radicals (methanol solution) and hydroxyl radicals (aqueous solution) in the samples was detected using electron paramagnetic resonance (EPR) spectra acquired on a spectrometer (JES-FA200, Bruker) using DMPO as a spin trapping agent.

**Photoelectrochemical measurements.** The CHI 660E electrochemical workstation (Shanghai Chenhua, China) with a three-electrode system in 0.5 M Na<sub>2</sub>SO<sub>4</sub> solution carried out the photoelectrochemical measurements. The prepared samples dispersed on the FTO (Fluorine-doped

tin oxide) conductive glass, Pt, and Ag/AgCl electrodes were used as working, counter, and reference electrodes. 10 mg of the photocatalysts were dissolved in ethanol (1 mL) and Nafion (5%, 20  $\mu$ L) solution, which was ultrasonically dispersed for 2 h. Then the FTO conductive glasses are covered with an appropriate amount of suspension. The EIS and photocurrent were also analyzed in 0.5 M  $\text{Na}_2\text{SO}_4$  solution under 300 W Xe light. PL (photoluminescence) was researched on a spectrofluorometer (Hitachi F-4600) with an excitation wavelength of 325 nm at ambient temperature. The in-situ DRIFT (in-situ diffuse reflectance infrared Fourier transform spectra) measurements were conducted using an FTIR (Fourier transform infrared spectrometer) spectrometer (Thermo, Nicolet iS 50) with an MCT detector. The spectra were presented in absorption units and obtained with a resolution of 4  $\text{cm}^{-1}$  after 64 scans. The reaction cell dome contained two ZnSe windows for IR transmission and a third window for irradiation, which was introduced through a liquid light guide connected to the same IR-light lamp. After degassing in an  $\text{N}_2$  atmosphere for 20 minutes, high-purity  $\text{CO}_2$  with pure water flowed through the reaction cell for 30 minutes, at which point the cell was sealed. Subsequently, FTIR spectra were recorded over time to study the dynamics of reactant adsorption in the absence of light and desorption/conversion under irradiation.

**DFT calculation.** The density functional theory (DFT) of the DMol<sup>3</sup> package in Materials Studio was applied to characterize the crystalline structure of  $\text{TiO}_2$ ,  $\text{BaTiO}_3$ , and heterojunction. The generalized approximation (GGA) with Perdew Burke Ernzerhof (PBE) was adopted to calculate all models. The energy cutoff was set as 5.8 eV. The convergence criterion for geometry optimization was set as Fine. 4 x 4 x 2 k-point grid was adopted for the electronic structure calculation. SCF tolerance was set as Fine ( $10^{-6}$ ).

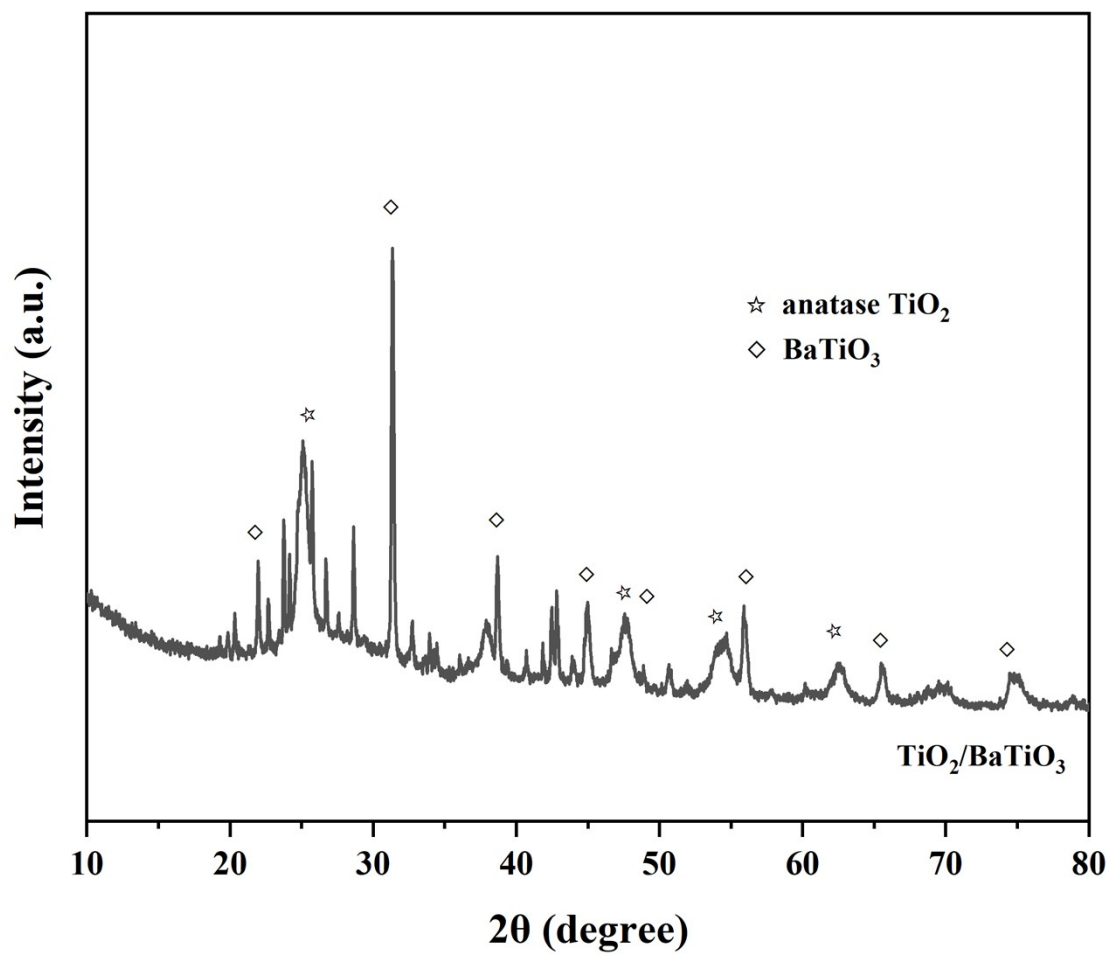
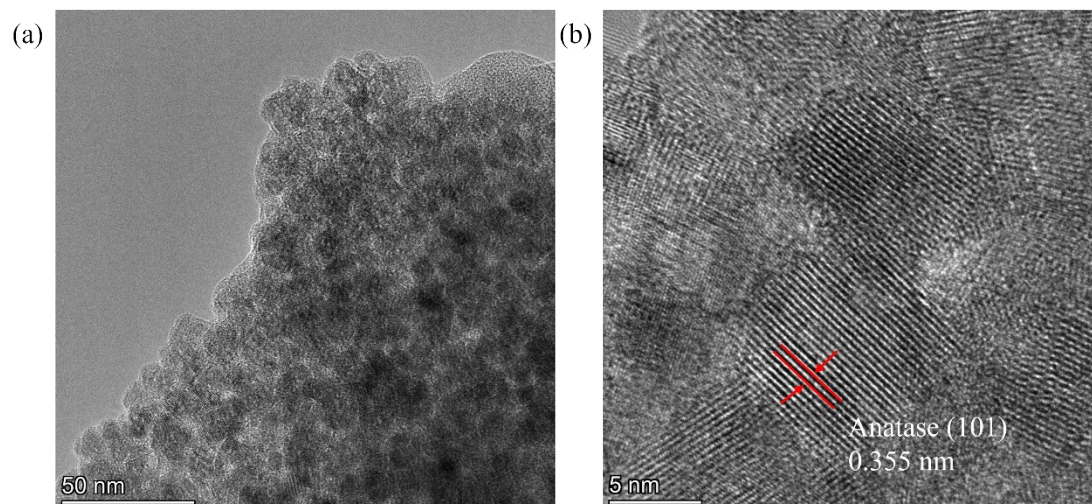
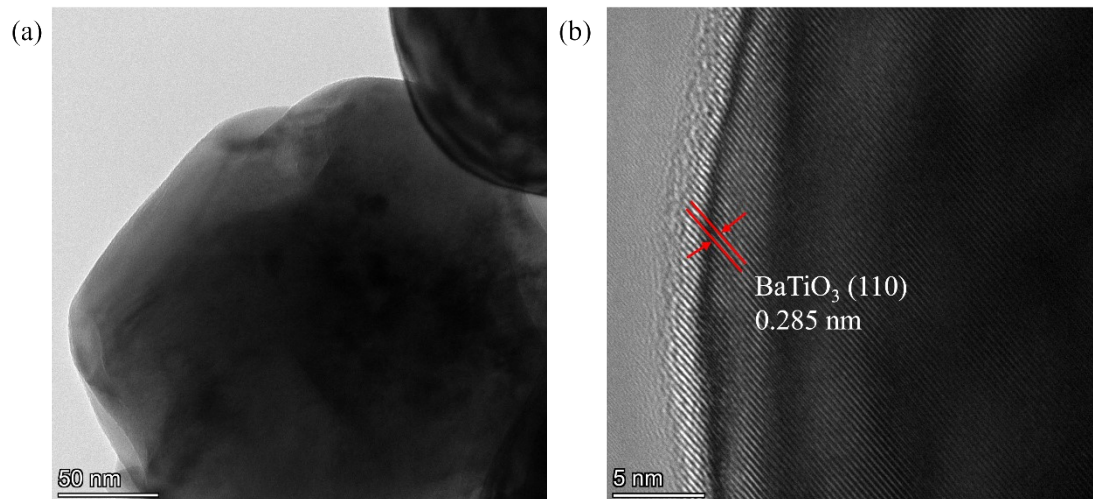


Fig. S1 The XRD pattern of  $\text{TiO}_2/\text{BaTiO}_3$



**Fig. S2** The TEM and HRTEM images of TiO<sub>2</sub>



**Fig. S3** The TEM (a) and HRTEM (b) images of BaTiO<sub>3</sub>

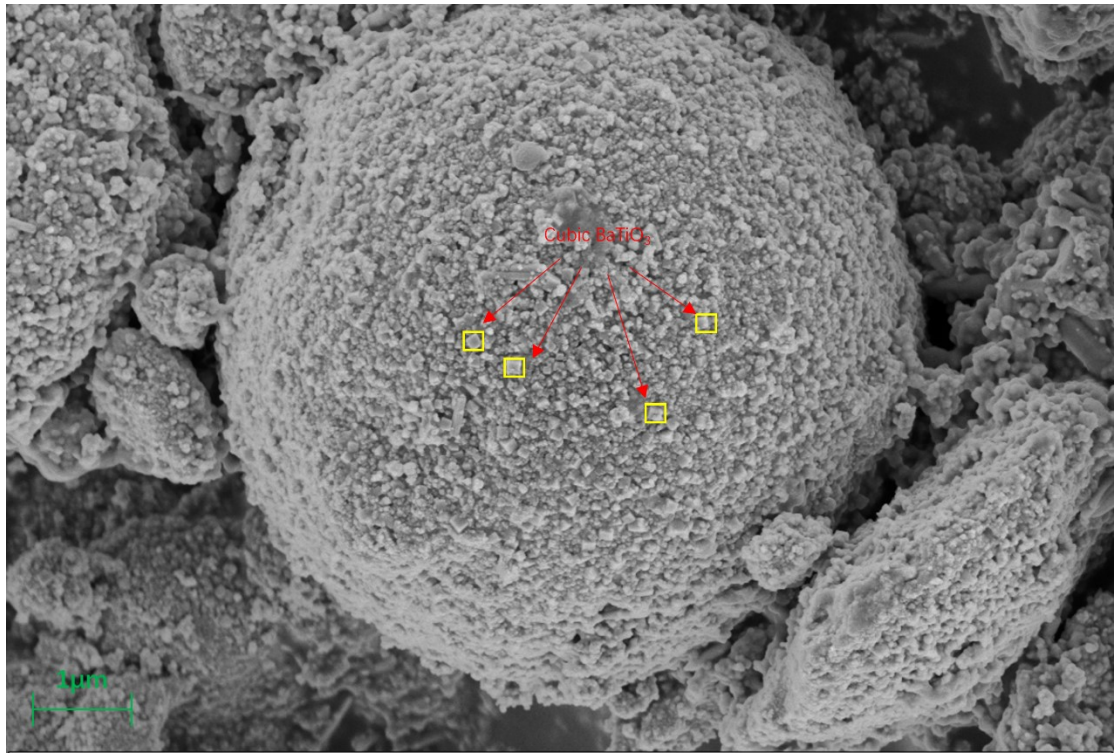


**Fig. S4** The SEM image of TiO<sub>2</sub>/BaTiO<sub>3</sub>

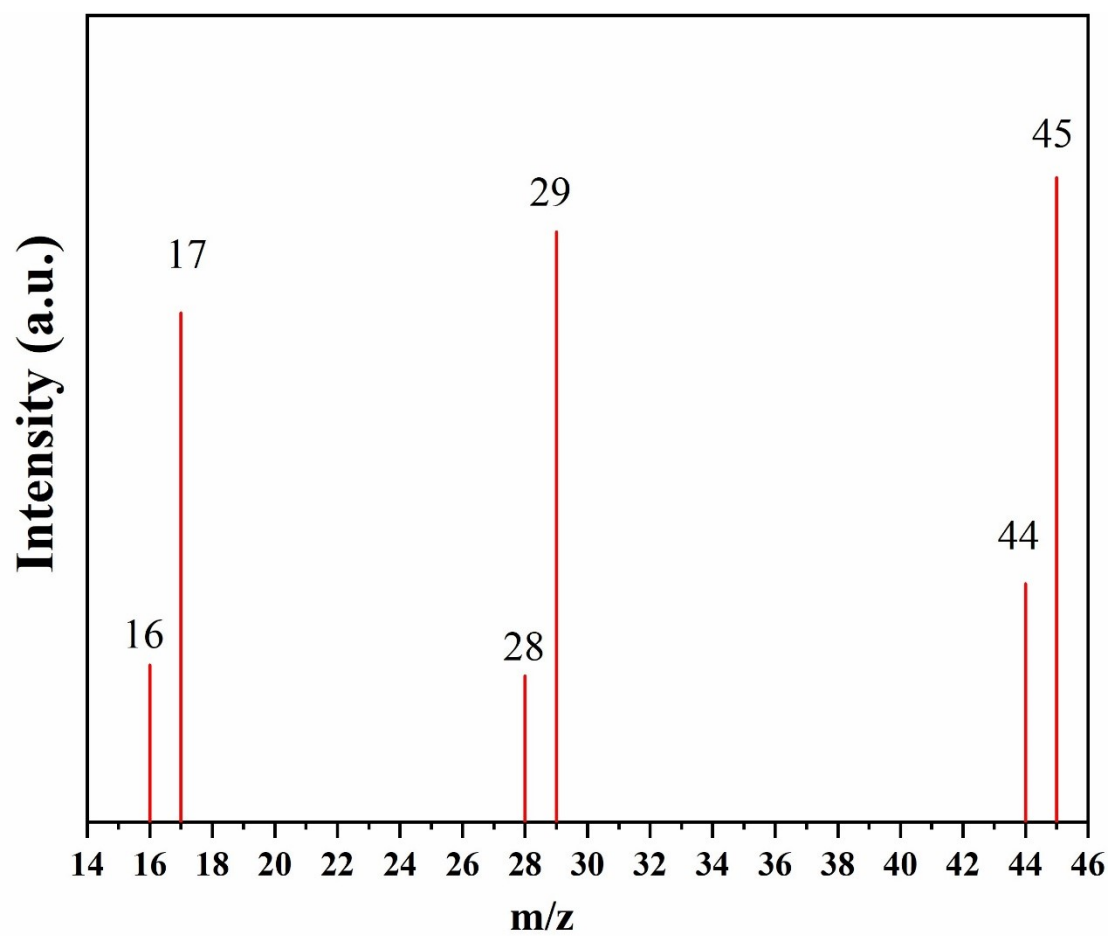
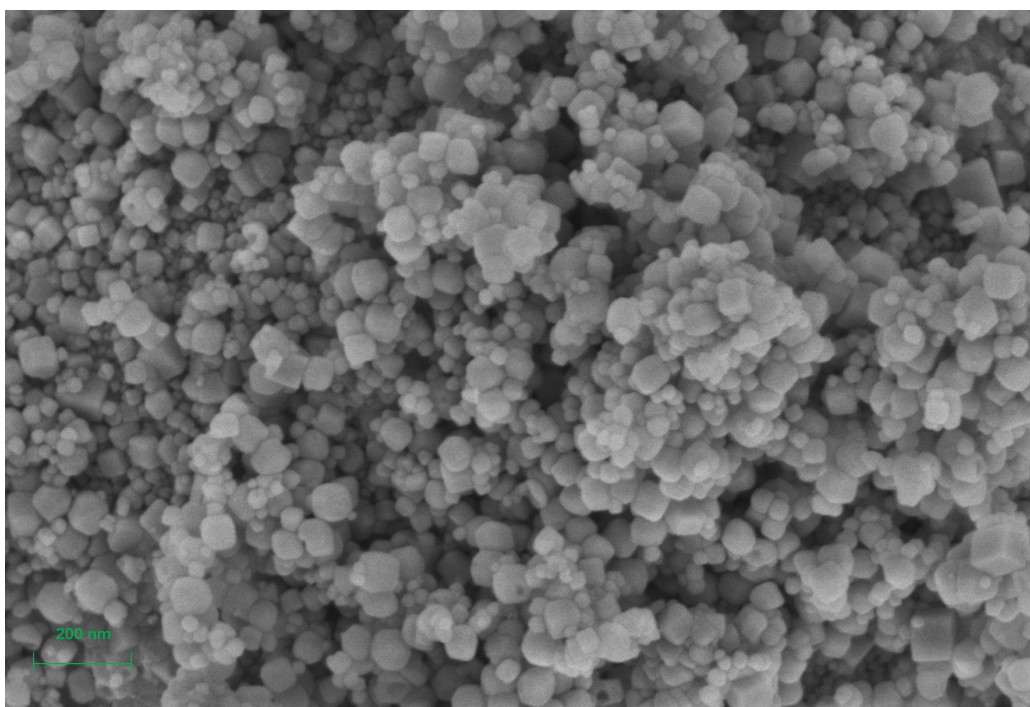


Fig. S5 Gas chromatography-mass spectrometry (GC-MS) of the products over 0.8BT.



**Fig. S6** The SEM image of 0.8TB after five consecutive cycles (30h).